Distribution of Cell in Mobile Network

Robert BESTAK

Department of Telecommunication Engineering, Faculty of Electrical Engineering, Czech Technical University in Prague, Technicka 2, 166 27 Prague, Czech Republic

robert.bestak@fel.cvut.cz

DOI: 10.15598/aeee.v13i4.1477

Abstract. *Femtocell concept has emerged as a cost-effective solution to manage indoor environment coverage and increasing capacity requirements. Compare to the conventional control macrocell deployment, femtocells are spread in the uncontrolled manner as they are deployed in network by customers themselves. This paper discusses multi-distance spatial analysis, Ripley's K function, to describe distribution of femtocells in a macrocell. In our study, we investigate various femtocell distributions and various numbers of femtocells in the macrocell.*

Keywords

Femtocells, mobile networks, Ripley's K function, simulations.

1. Introduction

Due to new range of applications, massive increase of connected devices and extended usage of video oriented applications, the traffic in mobile and wireless networks has significantly grown over the past years. Additionally, this trend is predicted to continue in the following years as well [1].

A possible cost-effective mean to deal with the traffic growth represents small cells such as femto, pico, or metro access points. The low-power access points enable to provide locally high capacity and data rates. This is applicable mainly in environments that are difficult to cover by traditionally macro base stations; for example houses, shopping malls, airports, railway stations, etc. Hereafter, we focus on the femtocell concept.

Femtocells can be seen as small cells covered by low-cost and low-power base stations typically deployed in network by customers themselves. These base stations are denoted as Femto Access Point, FAP, or using 3GPP notation as Home (evolved) NodeB, H(e)NB. The FAPs are connected to mobile operators' networks via subscribe lines that can be either wired or wireless; e.g. ADSLs, optics, WiFi, or nowadays even via satellites [2].

Compare to the conventional macro base stations, the number of operated FAPs within a mobile network can be very large. Therefore, to enable smooth and simple mass deployment of femtocells, a self-organizing concept has to be integrated in FAPs. Customers cannot be expected to have whatever knowledge how to install and how to configure FAPs; the whole configuration process has to be done automatically by FAPs themselves and/or under the network assistance.

The market status, the recent advances in algorithmic design and the ongoing standardization efforts for femtocells is presented in [3]. The technical impact and the business models of the various access control methods for femtocells are discussed in [4], while a wide range of radio resource allocation and power control techniques for cross-tier interference mitigation are included in [5], [6]. Various studies have addressed the issues such as energy saving [7], [8], interference mitigation [9], [10], location management [11], handover issues [12], [13], or performance analysis [14], [15].

In case of highly populated metropolises a quite high number of FAPs can operate under coverage of one macro base station. Due to customer self-deployment manner, a mobile operator has no real knowledge about placement or about at least sort of distribution of FAPs in its network (see Fig. 1). Having such sort of information would allow an operator to take proactive steps to manage better the "uncontrolled" deployment of FAPs by its customers, e.g. by allocating suitable predefined frequencies or physical cell identifier to FAPs.

In this paper, multi-distance spatial cluster analysis, Ripley's K function, to characterize the distribution of FAPs in the macrocell is studied. We discuss different possibilities of FAPs deployment such as random,

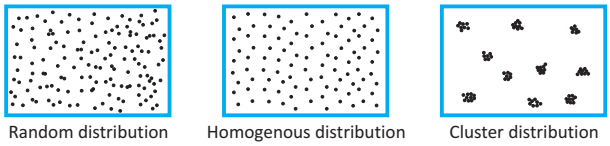

Fig. 1: Example of distributions of FAPs in a macrocell.

homogenous, in clusters and by taking into account different number of FAPs in our study.

The rest of paper is organized as follows. The next section provides brief overview the Ripley's K function. Simulation model and obtained results are discussed in Section 3. . Finally, Section 4. concludes the paper.

2. Ripley's K Function

The Ripley's K function represents a tool to analyze completely mapped spatial point process data which consist of location events. These are usually recorded in two dimensions, but they may be locations along a line or in space. Here, we focus on two-dimensional spatial data scenario. Applications can include for example spatial patterns of trees [16], bird nests [17], disease cases [18], etc.

The K function is given as [19]:

$$K(r) = \lambda^{-1} E(r), \tag{1}$$

where $K(r)$ describes characteristics of the point processes at many distance scales and λ is the event density (i.e. in our case FAPs per unit area) and can be written as:

$$\lambda = \frac{N}{A}, \tag{2}$$

where N represents the observed number of points and A is the area of study region, i.e. in our case one macrocell.

The $E(r)$ is the expected number of points (FAPs) within a distance r (Ripley's radius) and is calculated by using the following equation:

$$E(r) = \frac{1}{N} \sum_{k=0}^{N} I_k(r), \tag{3}$$

where $I_k(r)$ is the number of points within a circle delaminated by radius r and centered at a point k.

Given the locations of all FAPs within a macrocell, how can $K(r)$ be estimated? $K(r)$ is a ratio of a numerator and the density of events, λ. The density, λ can be estimated using Eq. (2). It is customary to condition on N, so the uncertainty in λ can be ignored, although unconditionally unbiased estimators have been suggested [20]. If edge effects are ignored, the numerator can be estimated as:

$$\frac{A}{N^2} \sum_{k=0}^{N} I_k(r). \tag{4}$$

However, the boundaries of the study area are usually arbitrary. Edge effects arise because points outside the boundary are not counted in the numerator, even if they are within distance r of the study area (see Fig. 2).

A variety of edge-corrected estimators have been proposed. The most commonly used one is [19]:

$$K(r) = \frac{A}{N^2} \sum_{k=0}^{N} \frac{I_k(r)}{w_k}, \tag{5}$$

where $0 \leq r \leq 0.3\sqrt{A}$ (the restriction on r is necessary because the corrector factor w_k can become very small when r increases, which would characterize the distribution on a similar scale in the study area). The factor w_k is the proportion of the circumference of the circle included in the study area A. The effects of edge corrections are more important for large r because large circles are more likely to be outside the study area A. Other edge corrected estimators have been proposed for example in [21]. Although $K(r)$ can be estimated for any r, it is common practice to consider r less than one-half of the shortest dimensions of the study area, if the study area is approximately rectangular.

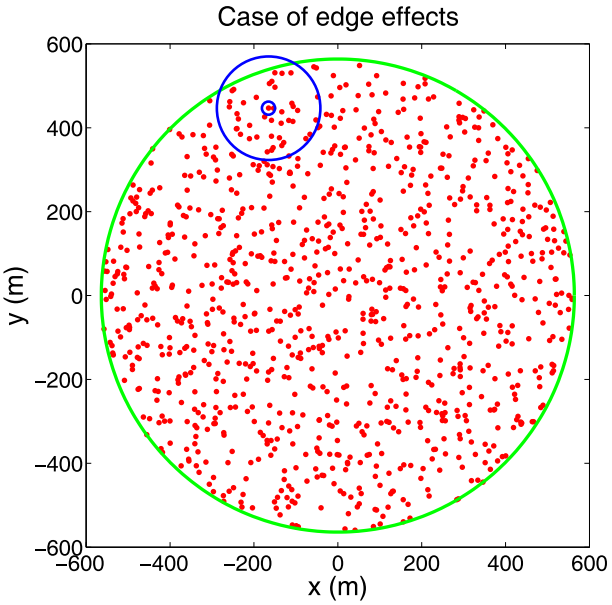

Fig. 2: Example of edge effects.

The correction of edge effects method proposed by Ripley consists to estimate the expected number of neighbors Ai which are outside of this area, for each distance r. The corrector factor can be calculated as:

$$w_k = \frac{2\pi - \alpha_{out}}{2\pi}, \tag{6}$$

where λ_{out} is given as:

$$\alpha_{out} = 2 \arccos\left(\frac{R_m^2 - d^2 - r^2}{2rd}\right), \qquad (7)$$

where R_m is macrocell radius and d is distance of the studied point, k, from the macro base station.

3. Performance Evaluation

3.1. Simulation Model

In our study, we assume a model consisting of one macrocell and set of FAPs, N. The femtocells may overlap to each other. The macrocell's radius, R_m, is set to 564 m (i.e. the covered area equals to 1 km^2) and the femtocell's radius, $R_F = 10$ m. The Ripley's K function is calculated using the Eq. (5).

Parameters used in simulations and their values are summarized in Tab. 1.

Tab. 1: Parameters and used values in simulations.

Parameters	Notations	Values
Number of FAPs	N	100–7000
Macrocell radius (macrocell surface)	R_m	564 m (1 km^2)
Femtocell radius	R_F	10 m
Ripley's radius	r	30–350 m

The FAPs are placed in the macrocell considering three distributions: a) random, b) homogenous, and c) cluster. In the analysis, different number of FAPs and clusters are taken into account. To simplify analysis, all clusters have same cluster sizes. An example of FAP distributions within the macrocell is shown in Fig. 3 and Fig. 4.

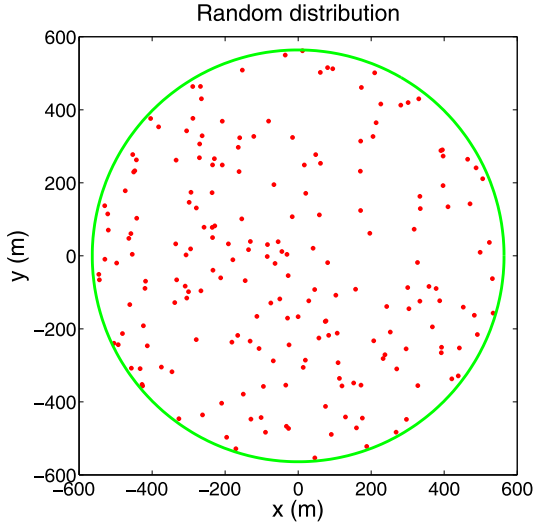

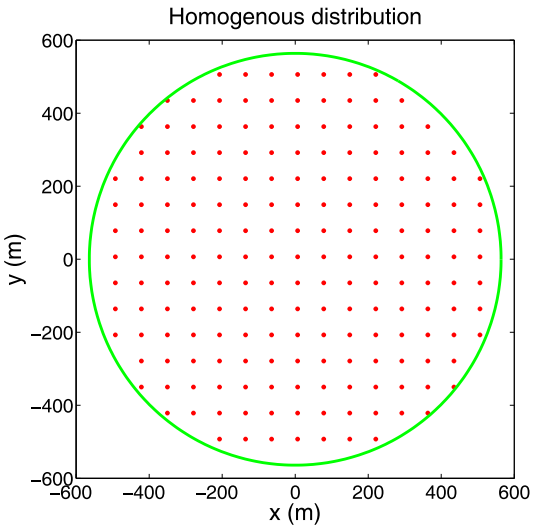

Fig. 3: Example of random and homogenous distribution of FAPs, $N = 200$.

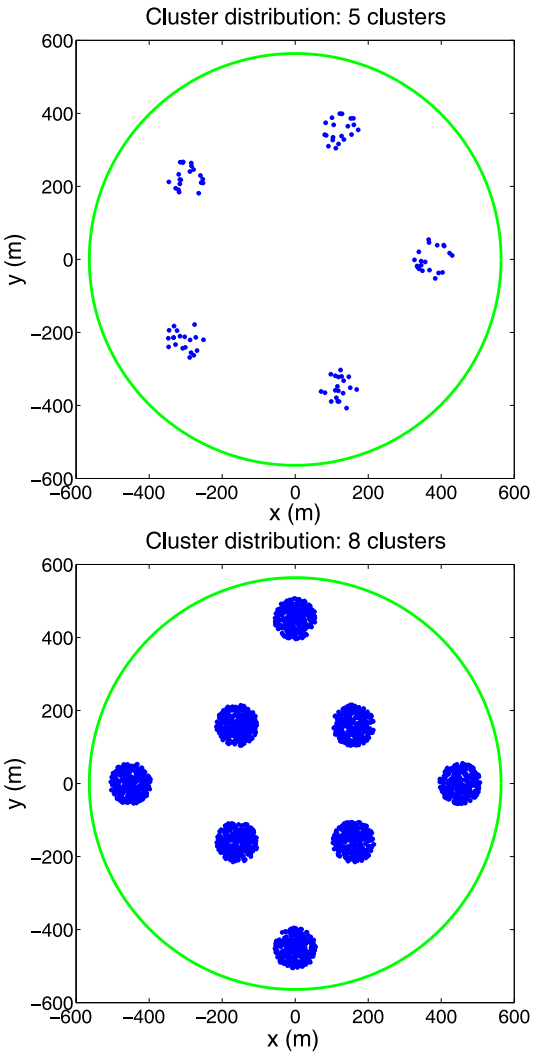

Fig. 4: Example of distribution in clusters; a) $N = 20$ per cluster, b) $N = 300$ per cluster.

3.2. Results

Figure 5 shows the course of K function for all three distributions where $N = 500$ and 3 clusters ($N = 500$ per cluster). Notice that in case of homogeneous Poisson process (also known as complete spatial randomness) of FAPs, the K function equal to πr^2 (see the green line in Fig. 5). This figure takes into account the edge effects that are corrected using Eq. (6). To illustrate the issue of edges, Fig. 6 shows how the results change when neglecting the edge effects. Mainly in case of random and homogenous distributions, we can observe the decrease of values.

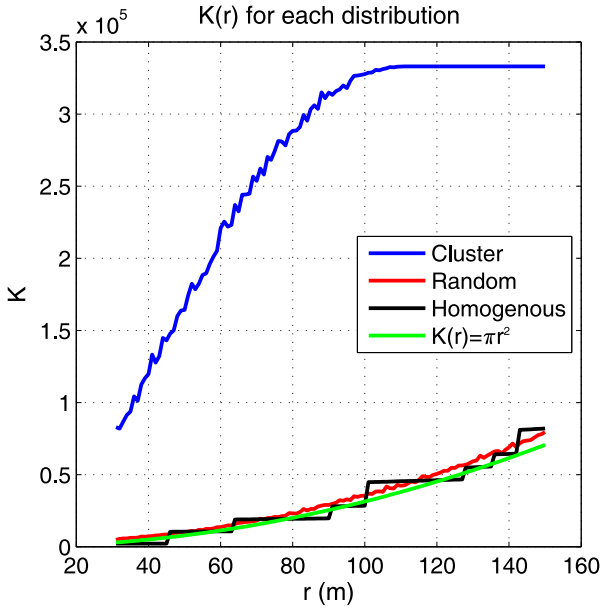

Fig. 5: K function for various distribution when correcting the edge effects, $N = 500$.

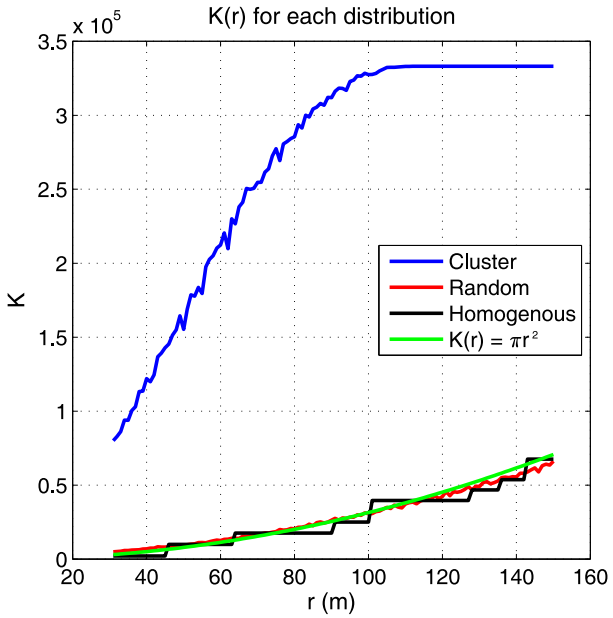

Fig. 6: K function for various distribution without corecting the edge effects, $N = 500$.

Figure 7 illustrates the K function for the random distribution when considering various numbers of FAPs. We can observe that the curves become smoother and approaching more and more the curve $K(r) = \pi r^2$, as the number of FAPs in the macrocell grows.

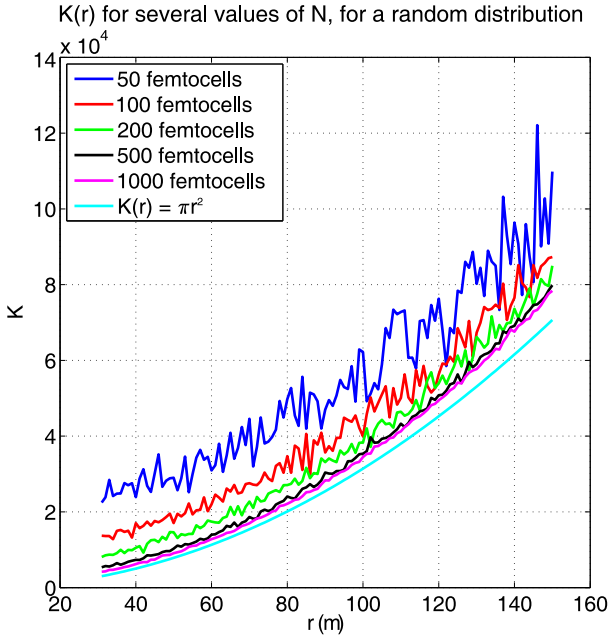

Fig. 7: K function for various number of FAPs and random distribution of FAPs.

Figure 8, resp. Fig. 9, illustrate the K function for different number of clusters when considering low and high number of FAPs per cluster ($N = 10$, resp. $N = 300$); the FAPs are distributed randomly inside a cluster. For higher number of FAPs, the curves become smoother.

We can observe that the K function increases until reaches a certain value of r, i.e. until r reaches the cluster radius (r'). For example, in case of 3 clusters, $r' = 100$ m. Further increase of r do not results in any increase of K function until the size of r does not reach another cluster (r'') and its FAPs, e.g. in case of 3 clusters, $r'' = 360$ m. Knowing these two points, we can simply calculate distance between the clusters, $d_{clus} = r''$ - $r' = 260$ m. This corresponds to the value used in our simulation when generating clusters within the macrocells. In the same way, we can find distances between clusters for the other curves. The distances between clusters based on Fig. 9 are summarized in Tab. 2.

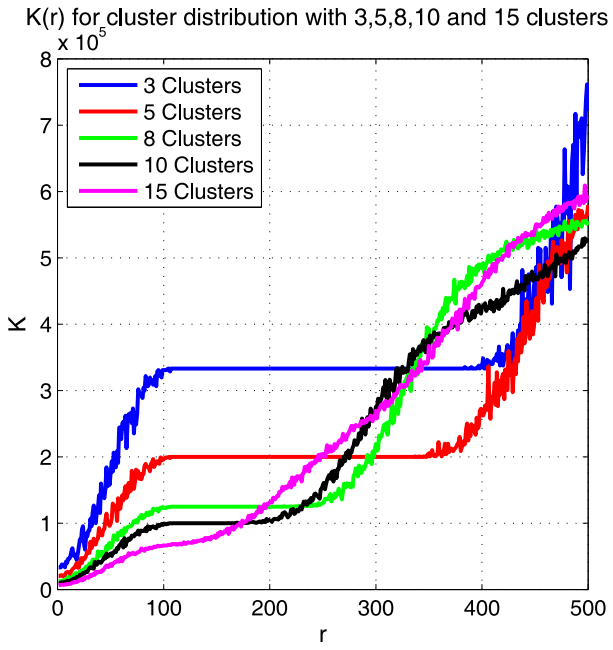

Fig. 8: K function for cluster distribution; $N = 10$ per cluster.

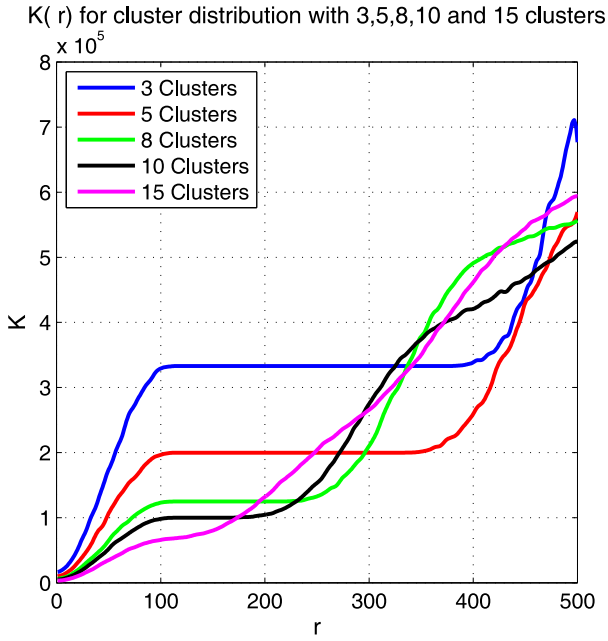

Fig. 9: K function for cluster distribution; $N = 300$ per cluster.

Tab. 2: Distances among clusters based on Fig. 9.

Number of clusters	r'	r''	d_{clus}
3	100 m	390 m	290 m
5	100 m	360 m	260 m
8	100 m	250 m	150 m
10	100 m	200 m	100 m
15	90 m	150 m	60 m

As the number of clusters in the macrocell increases and thus the distance between them decreases, the cluster distribution slowly approaching the random distribution.

Notice that the growth of curves for $r > r''$ can be faster than in the range $r < r'$ as there can be more than one cluster in the range $r'' > r$ (see for example the 10 clusters curve in Fig. 9).

4. Conclusion

In this paper, we discuss multi-distance spatial analysis, using Ripley's K function, to characterize distribution of FAPs in one macrocell. We analyze the variation of K function for random, homogenous and cluster distribution of FAPs and for different numbers of FAPs and clusters per macrocell. We also illustrate the edge effect on the K functions.

In the next work, we plan to characterize the distributions of FAPs using the linearized form of Ripley's K-function, called Besag's L function.

Acknowledgment

This research work was supported by the Grant Agency of the Czech Technical University in Prague, grant no. SGS13/199/OHK3/3T/13.

References

[1] QUALCOMM. The 1000x Mobile Data Challenge. *Qualcomm Technologies, Inc.* [online]. 2012. Available at: `https://www.qualcomm.com/invention/1000x`.

[2] BRIGHT, J. and D. MAVRAKIS. Satellite backhaul for rural small cells. *Informa telecoms & media* [online]. 2012. Available at: `http://www.informatandm.com/wp-content/uploads/2012/04/iDirect-White-Paper_online.pdf`.

[3] ANDREWS, J. G., H. CLAUSSEN, M. DOHLER, S. RANGAN and M. C. REED. Femtocells: Past, Present, and Future. *IEEE Journal on Selected Areas in Communications*. 2012, vol. 30, iss. 3, pp. 497–508. ISSN 0733-8716. DOI: 10.1109/JSAC.2012.120401.

[4] DE LA ROCHE, G., A. VALCARCE, D. LOPEZ-PEREZ and J. ZHANG. Access Control Mechanisms for Femtocells. *Communications Magazine.*

2010, vol. 48, iss. 1, pp. 33–39. ISSN 0163-6804. DOI: 10.1109/MCOM.2010.5394027.

[5] SAQUIB, N., E. HOSSAIN, L. B. LE and D. I. KIM. Interference management in OFDMA femtocell networks: issues and approaches. *Wireless Communications*. 2012, vol. 19, iss. 3, pp. 86–95. ISSN 1536-1284. DOI: 10.1109/MWC.2012.6231163.

[6] LE, L. B., D. NAYATO, E. HOSSAIN, D. I. KIM, and D. T. HOANG. QoS-aware and Energy-Efficient Resource Management in OFDMA Femtocells. *IEEE Transactions on Wireless Communications*. 2012, vol. 12, iss. 1, pp. 180–194. ISSN 1536-1276. DOI: 10.1109/TWC.2012.120412.120141.

[7] BOUSIA, A., A. ANTONOPOULOS, L. ALONSO and C. VERIKOUKIS. Green Distance-Aware Base Station Sleeping Algorithm in LTE-Advanced. In: *IEEE International Conference on Communication (ICC)*. Ottawa: IEEE, 2012, pp. 1347–1351. ISBN 978-1-4577-2052-9. DOI: 10.1109/ICC.2012.6364240.

[8] CHEN, T., Y. YANG, H. ZHANG, H. KIM and K. HORNEMAN. Network Energy Saving Technologies for Green Wireless Access Networks. *Wireless Communications*. 2011, vol. 18, iss. 5, pp. 30–38. ISSN 1536-1284. DOI: 10.1109/MWC.2011.6056690.

[9] SUN, Y., R. P. JOVER and X. WANG. Uplink Interference Mitigation for OFDMA Femtocell Networks. *IEEE Transactions on Wireless Communications*. 2011, vol. 11, iss. 2, pp. 614–625. ISSN 1536-1276. DOI: 10.1109/TWC.2011.120511.101794.

[10] PARK, S., W. SEO, Y. KIM, S. LIM and D. HONG. Beam Subset Selection Strategy for Interference Reduction in Two-Tier Femtocell Networks. *IEEE Transactions on Wireless Communications*. 2010, vol. 9, iss. 11, pp. 3440–3449. ISSN 1536-1276. DOI: 10.1109/TWC.2010.092410.091171.

[11] FERRAGUT, J. and J. MANGUES. A Self-Organized Tracking Area List Mechanism for Large-Scale Networks of Femtocells. In: *IEEE International Conference on Communication (ICC)*. Ottawa: IEEE, 2012, pp. 5129–5134. ISBN 978-1-4577-2052-9. DOI: 10.1109/ICC.2012.6363731.

[12] XENAKIS, D., N. PASSAS and C. VERIKOUKIS. A novel handover decision policy for reducing power transmissions in the two-tier LTE network. In: *IEEE International Conference on Communication (ICC)*. Ottawa: IEEE, 2012, pp. 1352–1356. ISBN 978-1-4577-2052-9. DOI: 10.1109/ICC.2012.6363941.

[13] YANG, G., X. WANG and X. CHEN. Handover Control for LTE Femtocell Networks. In: *International Conference on Electronics, Communications and Control (ICECC)*. Zhejiang: IEEE, 2011, pp. 2670–2673. ISBN 978-1-4577-0320-1. DOI: 10.1109/ICECC.2011.6067552.

[14] DHILLON, H. S., R. K. GANTI, F. BACCELLI and J. G. ANDREWS. Modeling and Analysis of K-Tier Downlink Heterogeneous Cellular Networks. *IEEE Journal on Selected Areas in Communications*. 2012, vol. 30, iss. 3, pp. 550–560. ISSN 0733-8716. DOI: 10.1109/JSAC.2012.120405.

[15] KIM, Y., S. LEE and D. HONG. Performance Analysis of Two-Tier Femtocell Networks with Outage Constraints. *IEEE Transactions on Wireless Communications*. 2010, vol. 9, iss. 9, pp. 2695–2700. ISSN 1536-1276. DOI: 10.1109/TWC.2010.070910.090251.

[16] PENTTINEN, A. and D. STOYAN. Recent Applications of Point Process Methods in Forestry Statistics. *Statistical Science*. 2000, vol. 15, no. 1, pp. 61–78. ISSN 2168-8745. DOI: 10.1214/ss/1009212674.

[17] GAINES, K. F., A. L. BRYAN and P. M. DIXON. The Effects of Drought on Foraging Habitat Selection in Breeding Wood Storks in Coastal Georgia. *Waterbirds: The International Journal of Waterbird Biology*. 2000, vol. 23, no. 1, pp. 64–73. ISSN 1938-5390.

[18] DIGGLE, P. J. and A. G. CHETWYND. Second-Order Analysis of Spatial Clustering for Inhomogeneous Populations. *Biometrics*. 1991, vol. 47, no. 3, pp. 1155–1163. ISSN 1541-0420. DOI: 10.2307/2532668.

[19] RIPLEY, B. D. The Second-Order Analysis of Stationary Point Processes. *Journal of Applied Probability*. 1976, vol. 13, no. 2, pp. 255–266. ISSN 0021-9002. DOI: 10.2307/3212829.

[20] DOGUWA, S. I. and G. J. UPTON. Edge-Corrected Estimators for the Reduced Second Moment Measure of Point Processes. *Biometrical Journal*. 1989, vol. 31, iss. 5, pp. 563–575. ISSN 1521-4036. DOI: 10.1002/bimj.4710310509.

[21] STOYAN, D. and H. STOYAN. *Fractals, Random Shapes and Point Fields: Methods of Geometrical Statistics*. Chichester: John Wiley and Sons Ltd, 1994. ISBN 978-0-471-93757-9.

About Authors

Robert BESTAK obtained a Ph.D. degree in Computer Science from ENST Paris, France (2003) and M.Sc. degree in Telecommunications from Czech Technical University in Prague, CTU, (1999). Since 2004, he has been Assistant Professor at Department of Telecommunication Engineering, Faculty of Electrical Engineering (FEE). His main research interests include 5G networks, big data in mobile network, and spectrum management. He is the Czech representative in the IFIP TC6 working group. He participated in several national, EU, and third party founded research projects.